Hybrid Technique for setting initial water saturation on core samples

Victor Fernandes[1,2,*], *Cyril* Caubit[1], *Benjamin* Nicot[1], *Fabrice* Pairoys[1], *Henri* Bertin[2] and *Jean* Lachaud[2]

[1]TotalEnergies CSTJF, Avenue Larribau, 64000 Pau, France
[2]I2M-Université de Bordeaux, CNRS, 351, Cours de la Libération, 33405 Talence, France

Abstract. Relative permeability and capillary pressure are important parameters in reservoir simulations because it helps in understanding and anticipating oil and/or gas production scenarios over the years. They are both obtained in laboratory after establishing the required initial conditions. As a matter of fact, before measuring imbibition relative permeability and capillary pressure, it is recommended to set initial rock reservoir conditions by establishing appropriate initial water saturation (Swi) and by ageing the core to restore the reservoir wettability. There are several conventional techniques to establish Swi. The Viscous Flooding is a fast technique, but it may create a non-uniform saturation profile and, in some cases, be inefficient to reach low Swi targets. Centrifugation is a capillary-driven technique that is also very fast, however the possibility of not desaturating the outlet face is a significant constraint. In both cases, reversing flow direction is generally performed to flatten the saturation profile, however this phenomenon is poorly controlled. The application of capillary pressure by Porous Plate allows targeting a specific value of Swi and generates a uniform saturation profile, however it is a very time-consuming method. In this paper we present the Hybrid Drainage Technique, which couples Viscous Flooding and Porous Plate approaches, significantly reducing the experimental duration when setting Swi. Another advantage of the method is the possibility of setting a uniform saturation profile at the targeted Swi. A specific core holder, adapted to NMR imaging, and allowing to perform both Viscous Flooding and Porous Plate testing without unloading the rock, was designed. Using this core holder enables performing ageing and imbibition coreflood testing, with no further manipulation of the core sample. Monitoring saturation profiles was made possible by using a NMR imaging setup. The method has been tested and validated on two outcrop samples from Bentheimer (sandstone) and Richemont (limestone), drastically reducing the experimental time of the primary drainage step in comparison to a classical Porous Plate drainage, but also leading to uniform water saturation profiles. The experiment duration is reduced, and it enables the realization of coreflooding, therefore this technique may be used for larger samples classically used in relative permeability experiments. This approach is preferred as it provides faster and more reliable measurements of saturation.

1 Background and state of the art

For the prediction of a hydrocarbon's reservoir production, numerical simulations are performed. The simulation models rely on two important petrophysical parameters: the relative permeability (Kr) and the capillary pressure (Pc). These are parameters that can only be obtained in the laboratory by performing Special Core Analysis (SCAL) studies. The workflow for the definition of both parameters contains several steps in which the original condition of the reservoir is expected to be reproduced as closely as possible to in situ conditions, in a technique known as wettability restoration.

The restored state method consists of coring a rock sample from the reservoir, sampling and plugging in the appropriate dimensions (usually cylindrical samples, varying from 1" and 1.5" in diameter and up to 3" in length [1]). The first step of the conventional procedure for reproduction of reservoir conditions consists in taking the sample to its initial state in terms of wettability. For that matter, the sample is cleaned with the objective of removing native oil, mud filtrates, precipitated salts and connate water. In this process, water, CO_2 and a variety of organic non-polar and polar solvents may be used to ensure appropriate cleaning intended to produce a water-wet sample. The sample is then submitted to conventional or vacuum oven-drying as well as flow through drying (by using, for instance, N_2).

The next step consists in setting the fluids' initial saturation. This phase is called primary drainage (PD) and mimics the migration phase of hydrocarbons from the source rock to the reservoir [2]. It begins with a fully brine-saturation state, followed by the injection of oil (in the case of an oil/water experiment). After reaching the target value of Swi, which is defined by the response of the reservoir logging relative to the region where the sample was cored, a wettability restoration phase is performed by ageing the core sample in its own crude oil at high temperature (typically 80°C) and pore (or back) pressure, which prevent water loss. After these steps, the sample may be considered as restored to its original state of wettability and fluid settings.

The following step is called imbibition, which consists in injecting brine in the core for oil recovery. This phase is performed to reproduce and experimentally simulate the production phase of the reservoir. During this phase, the oil production rate, the saturation profile dynamics and the pressure drop between the sample's inlet and outlet allow the determination of Kr and Pc by inverse analysis. However, any

* Corresponding author: victor.de-oliveira-fernandes@totalenergies.com

error committed when setting fluids initial saturation and restoring rock's wettability will impact the sample's response during imbibition, leading to uncertainties on Kr and Pc estimations.

As primary drainage is a key step in restoring the rock's true conditions in the reservoir, several techniques may be used, each of them carrying advantages and drawbacks. Variations have been proposed by different authors to benefit from the best features of each technique.

As all experimental steps in SCAL are supposed to reproduce the reservoir behaviour, experimental artefacts must be avoided. The main artefact impacting the establishment of a homogeneous Swi profile is capillary end effects (CEE) that is defined as a gradient of the wetting phase saturation along the sample longitudinal axis. This effect is originated from a capillary pressure drop between inlet and outlet faces of the sample during oil injection. It must be corrected before any SCAL tests as it does not represent a real behaviour of fluids during migration in the reservoir.

Because relative permeability and capillary pressure are related to fluid saturations in a non-linear way, the presence of a saturation gradient will prevent their direct determination. However, by means of numerical simulation based on an extended form of Darcy's law with appropriate boundary conditions, the effect of a non-uniform saturation profile on Kr and Pc determination may be mitigated [3, 4, 5, 6, 7].

Whereas the direct impact of CEE on the determination of Kr and Pc may be corrected, the impact of CEE on wettability restoration, thus on Kr and Pc calculation, is a more complicated issue. One of the hypotheses is that the wettability of the core is homogeneous, so that Kr and Pc will behave in the same way along the core. However, as wettability change during ageing is dependent on fluid saturations, a non-uniform wettability profile will result from a sample for which capillary end effects have not been removed [8]. Furthermore, maintaining a homogeneous saturation profile during ageing is a necessary but insufficient condition. It has been shown that a heterogeneous wettability profile may result even when a homogeneous saturation profile is ensured during ageing [9, 10].

Nonetheless, capillary end effects are not always a phenomenon that need to be minimized. Some experiments have been designed to take advantage of this effect, for example, to speed up the measurement of capillary pressure curve [11, 12, 13, 14].

There are three major primary drainage techniques in SCAL experiments, which main advantages and drawbacks are presented in Table 1:

Table 1 – Advantages and Drawbacks of PD techniques

	Advantages	Drawbacks
Viscous Flooding	Fast method	Non-uniform saturation profile
	Standard injection rig and equipment	Difficult to reach low Swi values
	Provides primary drainage Kr	Fines migration under high flowrate
Centrifuge	Faster than Porous Plate	Friable samples can be easily damaged
	Capillary pressure driven technique	Specific equipment needed
	Lower CEE than Viscous Oil Flooding	Manipulation needed for further SCAL steps
Porous Plate	Homogeneous saturation profile	Time consuming
	Good method for friable samples	Capillary contact may be a problem
	Capillary pressure driven technique	Manipulation needed for further SCAL steps

The principal technique used in SCAL experiments with large samples (typically D = 50 mm; L = 200 mm) is Viscous Oil Injection that consists in injecting oil at constant flowrate steps in the sample while measuring the pressure drop between inlet and outlet as well as fluid productions. At first, only water will be produced as oil percolates in the sample and expels water from the pores. After oil breakthrough, both phases will be produced until no more water is recovered. This is a fast technique that does not require any particular setup, being possible to be carried out in the same cell used for the following steps in SCAL (ageing and flooding) and by a simple injection rig. However, capillary end effects (CEE) due to the capillary pressure drop along the sample is an important constraint (as seen in Fig. 1), as well as reaching low values of Swi (<10%) in some specific cases. This problem may be solved by injecting at higher flowrates. Nonetheless, it may cause irreversible damage in the core, such as fines migration and additional pore volume creation, impacting further measurements once the rock matrix has been modified.

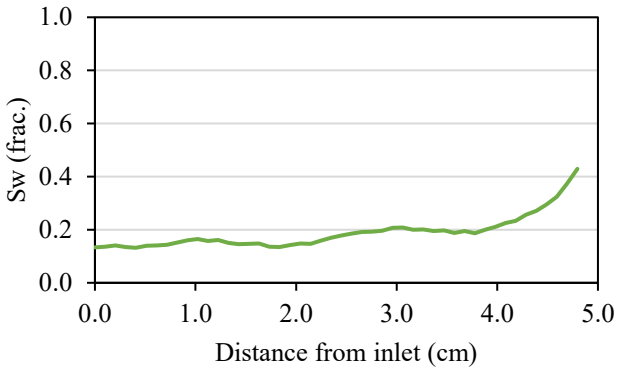

Fig. 1. Water saturation profile of a Bentheimer sandstone measured by NMR after a Viscous Flooding primary drainage. Capillary end effects are clearly visible close to the sample's outlet.

One method of dealing with capillary end effects is to reverse the direction of injection. Although this method may generate a homogeneous saturation profile, two major issues may result:

- Brine placed in the outlet of the sample is mobilized and displaced towards the inlet, generating an imbibition and increasing water saturation at these points. This phenomenon can be seen in Fig. 2.
- Formation of disconnected oil clusters that will adversely affect wettability restoration and impact effective permeability measurements [15].

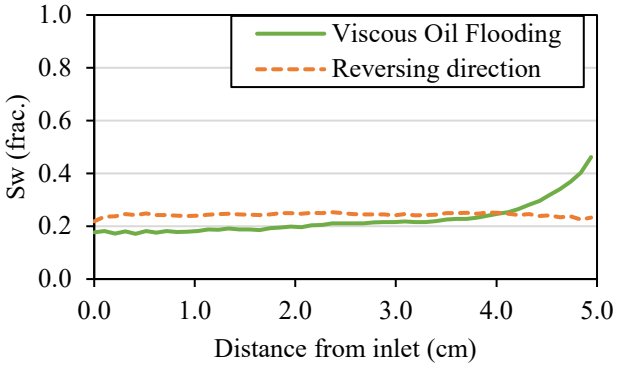

Fig. 2. Bentheimer sandstone submitted to Viscous Oil Flooding (VOF) followed by flow direction reversal – NMR profiles imaging. It is possible to observe a general imbibition of the brine present in the last cm after the last step of VOF (green line) on the final profile (orange-dotted line).

Centrifugation is another technique for setting initial oil saturation. This technique was introduced by Hassler and Brunner [16]. It consists in placing a rock sample inside a centrifuge machine that will induce an injection pressure through centripetal forces from high speed rotation. Ignoring any two dimensional effects, the expression that defines the capillary pressure at a radius r is given by Eq. 1:

$$P_c(r) = \frac{1}{2}\Delta\rho\omega^2\left(R^2 - r^2\right) \qquad (1)$$

where, P_c is the capillary pressure, $\Delta\rho$ is the density difference between the resident brine and the injected fluid, ω is the rotational speed of the centrifuge and R is the distance between the centrifuge central axis and the sample outlet.

The issues of this technique are not only the presence of capillary end effects (as seen in Fig. 3), but also the possibility of not desaturating the outlet face of the sample. This effect comes from the boundary condition when r is equal to R in Eq. 1, which gives $P_c = 0$, then, Sw = 1. The solution for these problems is to reverse injection direction; however, it potentially induces the same issues as presented for the viscous oil injection. In addition, by using Centrifuge as primary drainage method, manipulation is generally needed to unload the sample from the centrifuge machine and to load it into the cell adapted for further flooding, such as ageing and imbibition steps.

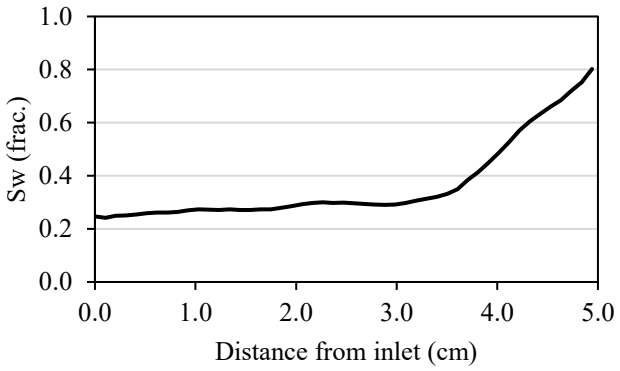

Fig. 3. Water saturation profile acquired by NMR after a Centrifuge primary drainage of a Bentheimer sandstone. Once again, the presence of CEE is clearly noticed close to the outlet.

The last fraction of the saturation profile in Fig. 1 and Fig. 3 showing an increase from 4 cm and 3.5 cm, respectively, is called the capillary foot. It is characterised as the remaining capillary end effect at the end of primary drainage for methods which do not prevent this effect by means of a semi-permeable membrane or plate.

The Porous Plate technique is considered the reference method for establishing initial water saturation. It was first introduced to measure capillary pressure versus water saturation in a water/gas system [17], further being extended to water/oil systems. This technique of primary drainage consists in placing a semi-permeable ceramic plate at the outlet of the sample. As a consequence of its small pore sizes and strong water-wetness, a high entry threshold pressure is needed for the non-wetting fluid to invade the ceramic. For a primary drainage cycle, the porous plate is essentially water-wet, allowing exclusively water to flow. The oil phase is directly injected by means of a volumetric pump, with continuous phase connection from the inlet to the porous plate. As capillary pressure is equally distributed along the sample, this technique generates a uniform saturation profile along the core, as seen in Fig. 4. However, as the porous plate permeability is extremely low to avoid oil invasion, this experiment may be highly time consuming depending on the targeted Swi. Another drawback is the need of unloading the porous plate from the overburden cell to perform further SCAL steps.

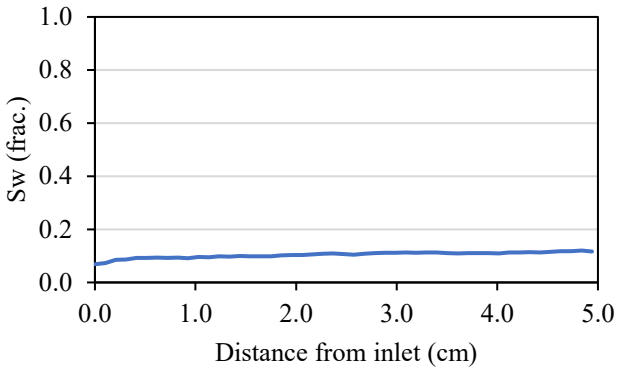

Fig. 4. Water saturation profile of a Bentheimer sandstone after a Porous Plate primary drainage. The profile, acquired by NMR imaging, shows a homogeneous saturation profile.

Some solutions to generate homogeneous saturation profile in reduced experimental time were proposed by some authors. The Spinning Porous Plate basically consists in placing a sample in contact with a multi-perforated porous plate to spin in a centrifuge [18]. It presents satisfactory results regarding the homogeneity of the saturation profile in sandstones of permeability around 70 mD at low Swi targets. However, it fails in achieving the same homogeneity quality for tighter samples and at higher levels of Swi. By performing the primary drainage cycle in the centrifuge, the following SCAL steps also demand additional handling. To overcome the combined issues of setting homogeneous profile and reducing handling, a by-pass to the porous plate was proposed [19] in the Toroidal Porous Plate. However, this proposition does not deal with experimental duration of the primary drainage step, as classic Porous Plate is performed in this case.

From these challenges, we propose a new Hybrid Drainage Technique (HDT) that is capable of not only reducing experimental time in comparison to a classic Porous Plate primary drainage, but also generating a homogeneous saturation profile without reversing flow direction as in Viscous Flooding and Centrifugation. By performing such a technique, we will prevent problems related to saturation profile heterogeneity, wettability restoration and disconnected oil clusters formation, as discussed earlier.

2 Methodology

2.1 The Hybrid Drainage Technique

The principle of the Hybrid Drainage Technique consists of coupling Viscous Flooding and Porous Plate for performing a fast, capillary-driven primary drainage, free from capillary end effects.

For this matter, the rock sample is inserted in an overburden cell together with a mono-perforated porous plate placed at the sample's outlet. This perforated porous plate is then mounted on a base-plate - called platen in what follows - constituted of two isolated outlets: one directly connected to the porous plate bypass (hereafter called Outlet 1), and one positioned immediately behind the porous plate (called Outlet 2). The presence of an O-ring ensures the isolation between both outlets that are connected to valves out of the cell.

The design of the overburden cell and the platen housing the porous plate, as well as the Hybrid Drainage Technique were filed for patent. A schematic drawing of the overburden cell is shown in Fig. 5.

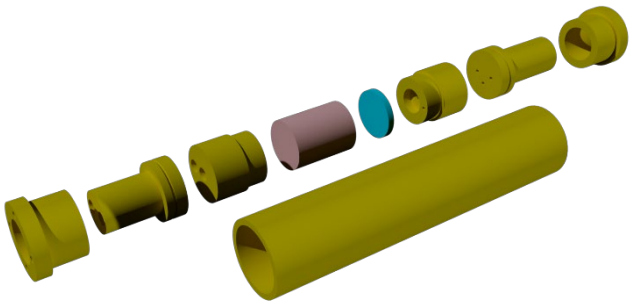

Fig. 5. Representation of the overburden cell.

As well as in other capillary-driven techniques (e.g., Porous Plate and Centrifuge) knowing the target Pc is mandatory for reaching a correct Swi value in the Hybrid Drainage Technique.

The HDT is composed of two phases: an initial oil injection similar to the Viscous Flooding technique and a second part similar to the Porous Plate technique, where capillary foot produced during Phase 1 will be eliminated.

Phase 1:

At first, oil is injected in the sample at constant pressure keeping Outlet 1 opened and Outlet 2 closed. Oil displaces water initially in place through the bypass of the porous plate (Outlet 1). This phase will generate a non-uniform saturation profile due to capillary end effects, such as in a classic Viscous Flooding. The end of Phase 1 is achieved when no more water is produced after oil breakthrough. At this moment, the goal is to minimise capillary foot by imposing a constant pressure on the whole sample that will homogenise fluid saturations, which will be performed in Phase 2.

Phase 2:

The transition to Phase 2 consists in swapping outlet's valves: Outlet 1, previously opened, is closed, and Outlet 2, previously closed, is opened. Therefore, a transition to a capillary-driven injection is initiated, where capillary pressure will be controlled by the porous plate. This will impose the same Pc along the core, eliminating the capillary foot. No modification is made regarding the injection pump once it is set in pressure regulation mode at the target inlet pressure. A schematic showing both outlets and the way they are distributed is shown in Fig. 6.

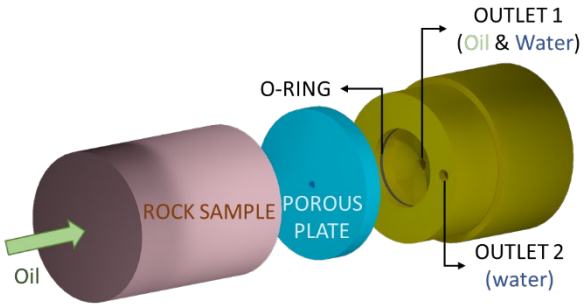

Fig. 6. Schematic representation of the method, showing both fluid outlets.

The main benefits of this technique are experimental time reduction and a homogenous saturation profile generation. The time reduction is due to fast water production from Viscous Oil Flooding while the latter results from a very quick transition to Porous Plate drainage without removal from the cell. In addition, the sample is immediately ready for further testing as it always remains in the experimental cell with confining stress.

2.2 Experimental Setup

The experimental setup used for performing HDT's proof of concept is shown in Fig. 7. The arrows indicate flow direction and fluid type in each line: red represents oil flow and blue represents brine flow.

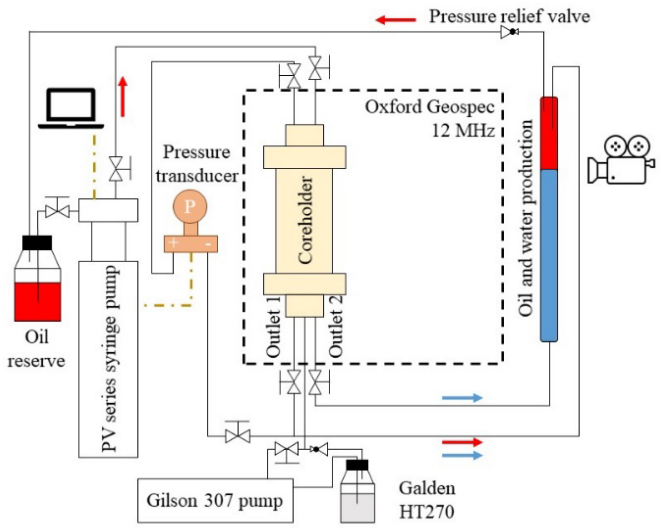

Fig. 7. Schematic of the experimental apparatus used for performing the HDT with *in situ* monitoring by NMR.

Oil injection was performed by a PV-Series low pressure syringe pump by FloxLab, which allows either constant flowrate or constant pressure fluid injection. The confinement pressure was maintained by a Gilson 307 pump directly connected to the overburden cell and to a pressure relief valve.

The NMR setup consists of a GeoSpec 12 MHz low-field DRX spectrometer by Oxford Instruments, equipped with magnetic field gradients on the vertical axis. This equipment allowed monitoring of saturation profiles and produced volumes during flooding by 1D saturation profiles and 1D T_2 relaxation times distribution NMR pulse sequences, respectively.

For double verification of produced volumes, a high-resolution camera is used for monitoring a graduated burette (± 0.03 cc) that receives volume production from the sample. A pressure reduction valve is placed downstream of the burette to keep the system under pressure during the experiment.

The overburden cell used for the experiments is metallic-free, being entirely made in PEEK®, as well as all flow lines. This is important as this material produces no NMR signal. The porous plate used for the experiments is made of porous alumina, with a typical pore radius of 90 nm.

2.3 Metrics used for comparing results

In order to perform a fair comparison between methods, metrics have been established for when water production during primary drainage would indicate the end of this step. For this matter, a sample is considered to have reached Swi when the rate of production is lower than 0.1 % per day.

Regarding the homogeneity of the saturation profile, a standard deviation of water saturation values in profiles was calculated after the end of each phase of primary drainage. In addition, a "max – min" parameter was established to indicate the maximum deviation in water saturation of a given profile.

3 Results

3.1 Solid and fluids properties

For the validation of this new method, cylindrical plugs (D = 38 mm per L = 50 mm) from two facies were chosen: Bentheimer sandstone (BEN) and Richemont limestone (RCH). The Richemont samples were extracted from the Thénac Block, which presents lower permeability and porosity compared to the conventional LCT block more commonly used in other works. For petrophysical characterisation, a Conventional Core Analysis (CCA) routine was performed and the results are shown in Table 2.

Table 2 - CCA data for Bentheimer and Richemont samples

Sample	Vp (Φ)	Kw
BEN-HD-LS	13.45 cc (23.69 %)	1832 mD
BEN-PP-LS	15.35 cc (26.94 %)	1857 mD
BEN-HD-HS	15.48 cc (27.22 %)	1996 mD
BEN-PP-HS	14.73 cc (25.35 %)	2034 mD
RCH-HD-LS	9.36 cc (16.38 %)	0.76 mD
RCH-PP-LS	8.94 cc (15.60 %)	0.78 mD
RCH-HD-HS	9.36 cc (16.38 %)	0.76 mD
RCH-PP-HS	9.95 cc (17.55 %)	0.80 mD

In order to allow an unambiguous detection of hydrocarbon by NMR, deuterium oxide (D_2O) was used for the aqueous phase since this fluid is not detected by NMR acquisitions. In addition, Potassium Iodide (KI) was added to the aqueous solution (7 wt.%) to improve the X-ray Micro-tomography imaging of the sample. Marcol-52, a synthetic oil manufactured by ExxonMobil, was used as non-wetting phase during primary drainage. Base properties of the fluids used in the experiments are presented in Table 3.

Table 3 - Basic properties of fluids used in experiments

Fluid	Composition	Density	Viscosity
Brine	D_2O + KI @ 70 g/l	1.16 g/cc	1.19 cP
Mineral Oil	Marcol-52	0.83 g/cc	12.00 cP

Furthermore, Galden HT270 fluorinated oil from Solvay was used as confinement fluid, as it produces no NMR signal.

3.2 Hybrid Drainage tests

In order to perform an exhaustive proof of concept of the Hybrid Drainage Technique, two Swi target values were defined for two rock samples with different scales of permeability – Low Swi (LS) and High Swi (HS) as in Table 2. Twin samples were submitted to the same levels of capillary pressure by the Hybrid Drainage Technique and by the conventional Porous Plate method – HD and PP in Table 2, respectively. In that way, a clear comparison of experiment duration between the HDT and PP primary drainage was achieved.

The Porous Plate experiments were performed in conventional Hassler Cells, and brine production was monitored by a burette connected to a pressure transducer that measures the pressure imposed by the produced brine column, which is then converted into a volume.

HDT tests were conducted in the new overburden cell suitable for NMR measurements. 1D T_2 relaxation times distribution allowed production monitoring and 1D saturation profiles provided the visualization of the saturation profile dynamics of the HDT. Furthermore, the latter showed the presence of capillary end effects at the end of Phase 1 and their elimination during Phase 2.

Both Porous Plate and HDT experiments were conducted at a confining pressure of 30 bar at ambient controlled temperature of 20 °C.

Moreover, a Darcy-scale simulation of the relative permeability and capillary pressure for the Richemont limestone during Phase 1 of the HDT was performed using CYDAR®. CYDAR® is a numerical simulator for design and interpretation of petrophysical laboratory experiments. It is a product from the French Institute of Petroleum and New Energies (IFPEN) and is commercialized by Cydarex.

3.2 High Swi (30 – 40%) Bentheimer sandstone

Taking into consideration Bentheimer's capillary pressure curve, as shown in Fig. 8, targeted Pc for high Swi in Bentheimer was set to Pc = 80 mbar.

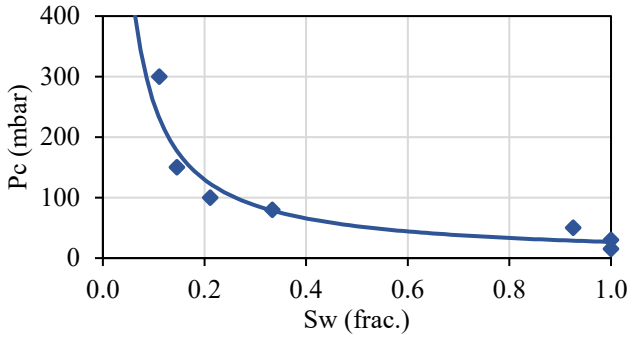

Fig. 8. Primary drainage Pc versus Sw curve for the Bentheimer sandstone.

In Fig. 9 it is possible observe water saturation profiles advancing at Phase 1 of the method.

At the end of this step, it's possible to notice the presence of the capillary end effect at the sample outlet originated from the pressure drop between inlet and outlet.

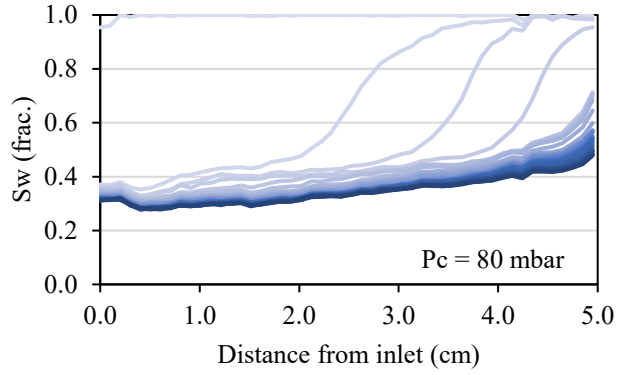

Fig. 9. Saturation profiles advancing during Phase 1 of BEN-HD-HS (Pc = 80 mbar).

At the end of this step, we observe for the water saturation profile:

- Std-dev (Sw): 4 %
- Max-min (Sw): 20 %

As no further motion was observed in saturation profiles, Phase 2 begins and water saturation profile dynamics are visible in Fig. 10. At this point, it is possible to notice more important changes in water saturation at the last fraction, as capillary pressure becomes homogeneous along the sample.

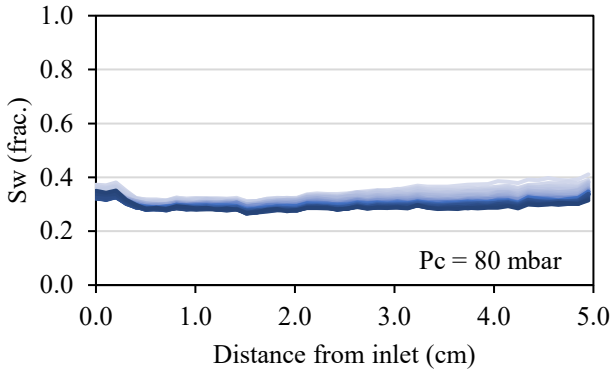

Fig. 10. Saturation profiles advancing during Phase 2 of BEN-HD-HS (Pc = 80 mbar).

At the end of the Hybrid Drainage Technique, we obtain:

- Std-dev (Sw): 1 %
- Max-min (Sw): 8 %

3.3 Low Swi (20 – 25%) Bentheimer sandstone

In order to reach a lower value of Swi in the Bentheimer sandstone, a Pc of 110 mbar was used. From Fig. 8, at this capillary pressure, Swi is around 22%. In Fig. 11 it is possible to observe a behaviour comparable to the behaviour of BEN-HD-HS (notation given by Table *2*), as an oil shock front invades the sample quickly desaturating it to a value close to Swi.

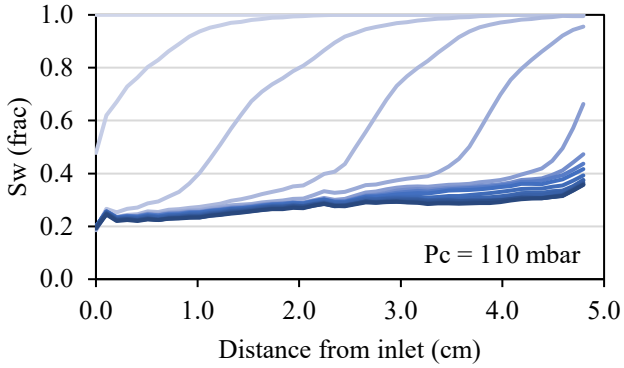

Fig. 11. Saturation profiles advancing during Phase 1 of BEN-HD-LS (Pc = 110 mbar).

At this point, we have:

- Std-dev (Sw): 3 %
- Max-min (Sw): 20 %

After transition to Phase 2, once again it is possible to observe a decrease in capillary end effects close to the outlet (Fig. 12).

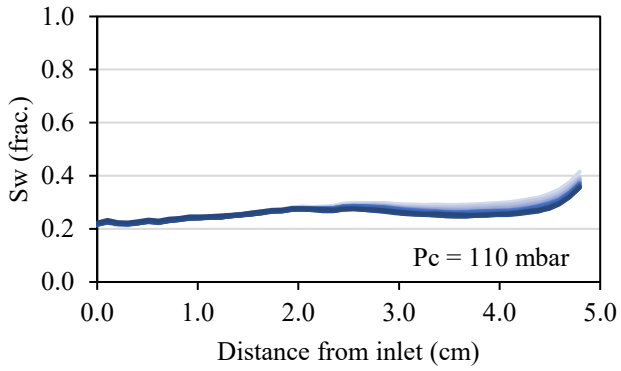

Fig. 12. Saturation profiles advancing during Phase 2 of BEN-HD-LS (Pc = 110 mbar).

At the end of the PD for BEN-HD-LS, we have:

- Std-dev (Sw): 2 %
- Max-min (Sw): 13 %

In Fig. 12 it is still possible to observe a small CEE in the last half cm of the sample. As fully saturated NMR imaging shows no abnormal saturation behaviour in this end, this effect does not represent a heterogeneity issue. Even though this test has respected the production cessation criteria, a longer Phase 2 would probably have homogenized the saturation profile, eliminating the CEE.

During Phase 1 of both experiments, it is possible to notice the shock front on the saturation profile as oil enters the sample at high velocity, quickly decreasing water saturation to a value close to Swi. It is also possible to observe a piston-like behaviour of the oil phase.

The monophasic dispersion allows the characterization of the dispersive behaviour of the porous media. This measurement consists of a miscible replacement of fluids, usually brines with different salinities (C the concentration of the injected brine and C0 the concentration of the resident brine). Density (or resistivity) is monitored downstream the sample during the experiment, which allows tracing the evolution of the relative concentration between the resident and the injected brine over time. Knowing the flowrate used for the experiment, it is possible to obtain the C/C0 versus injected Pore Volume (PV).

The behaviour of the monophasic dispersion curve of the Bentheimer sandstone [20], as observed in Fig. 13, is in good agreement with the saturation profiles dynamic during Phase 1 of HDT.

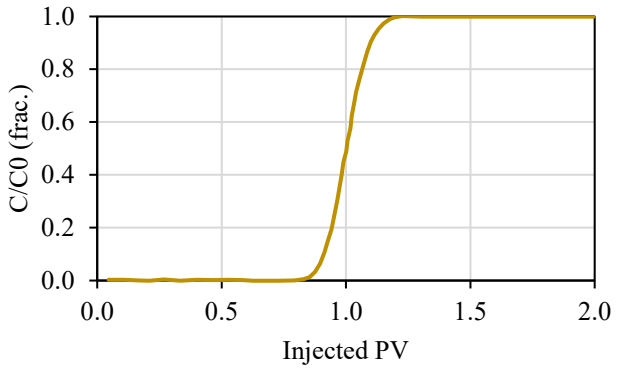

Fig. 13. Bentheimer's dispersion curve (extracted from Satken et al. 2021).

3.4 High Swi (40 - 45%) Richemont limestone

The Richemont Pc versus Sw curve is shown in Fig. 14.

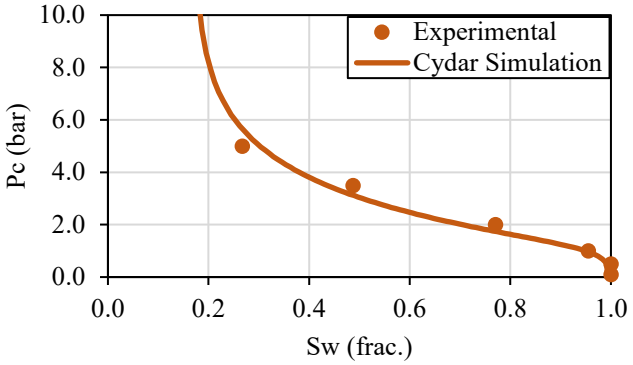

Fig. 14. Primary drainage Pc versus Sw curve for the Richemont limestone.

As the Richemont sample is a much less permeable rock, capillary pressure for high values (HS) of Swi was set to 3.875 bar.

In this case, Phase 1 was performed at a constant flowrate (Q = 3 cc/h), in order to allow the numerical simulations needed to infer Kr and Pc by inverse analysis. For that matter, the pressure drop between inlet and outlet, water production and Sw profiles advancing were measured. Sw profiles advancing are shown in Fig. 15.

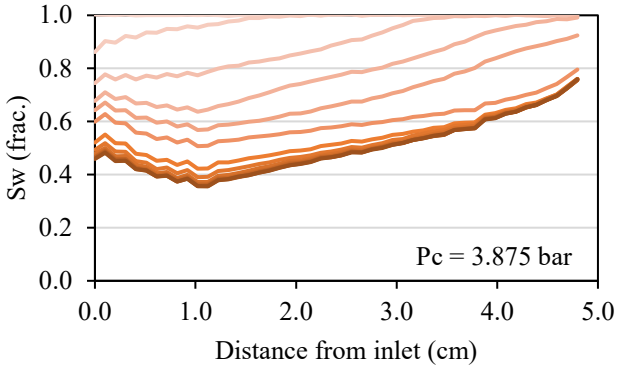

Fig. 15. Saturation profiles advancing during Phase 1 of RCH-HD-HS (Pc = 3.875 bar).

In the transition from Phase 1 to Phase 2, we had:

- Std-dev (Sw): 9 %
- Max-min (Sw): 40 %

After the transition to Phase 2, it was possible to observe the equilibration of the saturation profiles as capillary pressure was equalized along the sample (Fig. 16). However, an effect observed in the inlet of the sample was not corrected after the transition. This effect will be further discussed in the "Discussion" section.

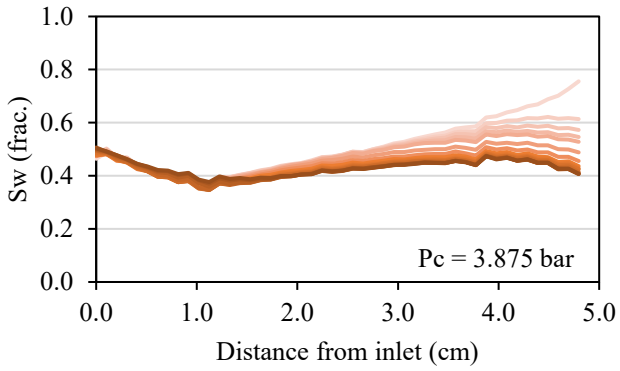

Fig. 16. Saturation profiles advancing during Phase 2 of RCH-HD-HS (Pc = 3.875 bar).

At the end of RCH-HD-HS primary drainage, we have:

- Std-dev (Sw): 2 %
- Max-min (Sw): 13 %

3.5 Low Swi (25 - 30%) Richemont limestone

Observing the Pc versus Sw curve for the Richemont sample, in order to achieve a Swi of around 25 %, a Pc of 5 bar was applied. Therefore, Phase 1 has been performed at a constant inlet pressure of 5 bar with open bypass, and the saturation profiles advancing may be seen in Fig. 17.

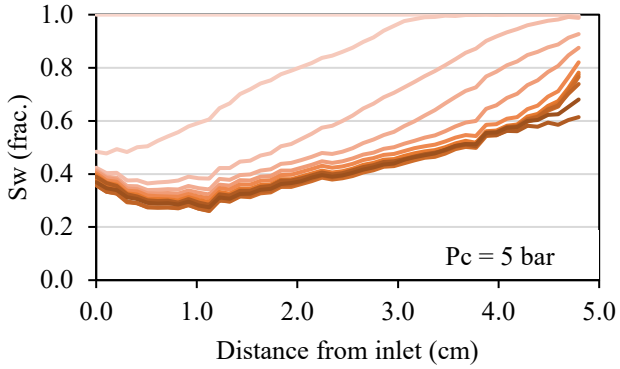

Fig. 17. Saturation profiles advancing during Phase 1 of RCH-HD-LS (Pc = 5 bar).

After Phase 1 of RCH-HD-LS primary drainage:

- Std-dev (Sw): 10 %
- Max-min (Sw): 41 %

After closing the bypass and performing the transition to Phase 2, a clear homogenization of the saturation profiles is observed in Fig. 18 by the elimination of the CEE. Nonetheless, the same effect in the saturation profile close to the inlet, as observed in the RCH-HD-HS, is present for this sample.

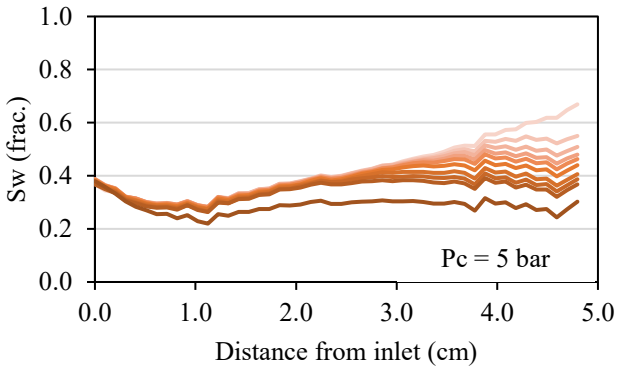

Fig. 18. Saturation profiles advancing during Phase 2 of RCH-HD-LS (Pc = 5 bar).

At the end of Phase 2, we have:

- Std-dev (Sw): 2 %
- Max-min (Sw): 16 %

In the Richemont case, the saturation profile dynamics behaves differently from Bentheimer's, as an earlier breakthrough and a much more dispersive behaviour takes place. This phenomenon was expected from the dispersion test presented in Fig. 19.

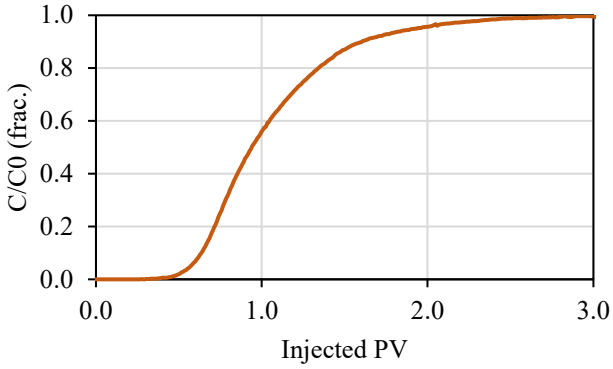

Fig. 19. Monophase dispersion for the Richemont sample.

3.6 Experimental time saving between HDT and Porous Plate

In this section, we present a comparison between the duration of the Hybrid Drainage Technique tests and the associated Porous Plate tests. The aim is to show the potential time reduction by using this technique over the classical Porous Plate.

As discussed before, equivalent Porous Plate tests were conducted by imposing the same inlet pressure in Bentheimer and Richemont sister plugs. Bentheimer's and Richemont's Sw versus time curves are shown in Fig. 20 and Fig. 21.

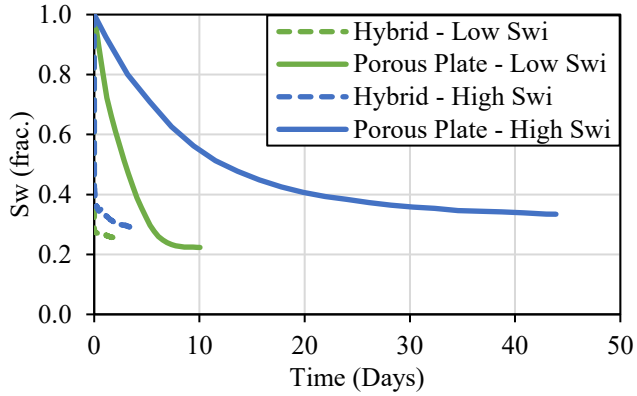

Fig. 20. Comparison between experimental duration for Porous Plate and Hybrid Drainage Technique on Bentheimer samples.

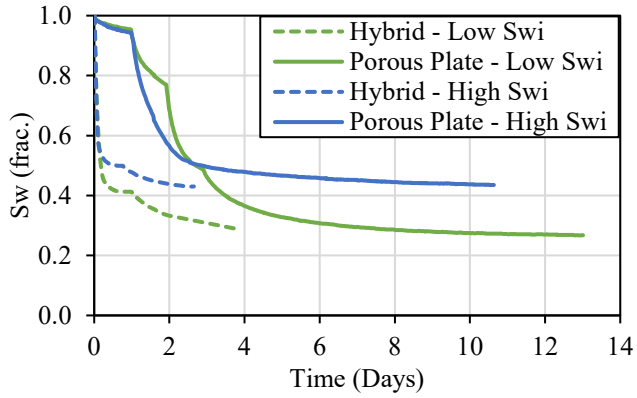

Fig. 21. Comparison between experimental duration for Porous Plate and Hybrid Drainage Technique on Richemont samples.

3.7 Simulation

A history match of the pressure drop (dP), water production (Vw) and Sw profiles was performed for the Richemont sample to define primary drainage Kr and Pc curves. The results are presented in Fig. 22, Fig. 23 and Fig. 24.

In addition, a Mean Absolute Percentage Error (MAPE) between the experimental data and the simulated results is presented for dP, water production and Sw profiles. This approach allows a validation of the match quality between experimental and simulated results. For calculating the MAPE, Eq. 2 was used:

$$\text{MAPE}\ (\%) = 100 * \frac{1}{N} * \sum_{i=1}^{N} \left| \frac{x_{exp} - x_{sim}}{x_{exp}} \right| \qquad (2)$$

where N is the number of experimental and simulated points compared, x_{exp} are each experimental point and x_{sim} are each simulated point.

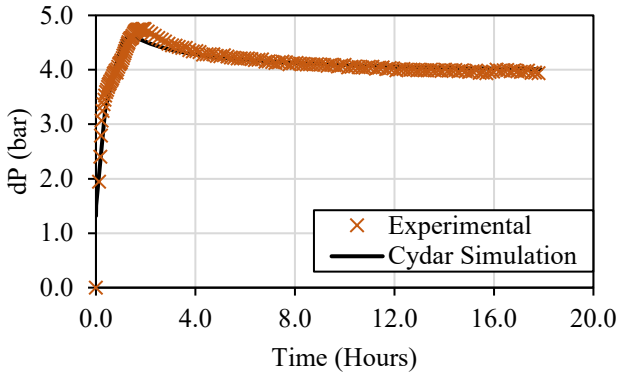

Fig. 22. History match of the pressure drop of the Richemont sample during Phase 1 of HDT.

- MAPE (dP): 1.9 %

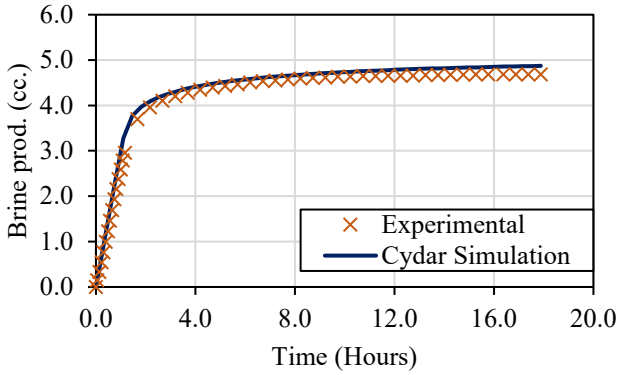

Fig. 23. History match of the produced brine volume of the Richemont sample during Phase 1 of HDT.

- MAPE (Vw production): 3.0 %

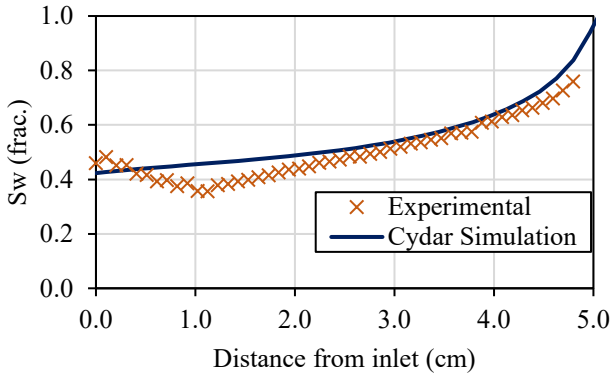

Fig. 24. History match of the water saturation profile imaged by NMR of the Richemont sample during Phase 1 of HDT.

- MAPE (Sw Profile): 8.5 %

Furthermore, Kr and Pc curves were obtained by optimization of the three parameters presented above and follow analytical functions of Corey and Logbeta, respectively.

Corey expressions [21] are useful for describing the relative permeability behaviour between residual end points

based on normalised phase saturation. In the case of primary drainage, the normalised oil relative permeability is defined by Eq. 3:

$$k_{ron} = S_{on}^{No} \quad (3)$$

The analogous equation for the water phase is given by Eq. 4:

$$k_{rwn} = S_{wn}^{Nw} \quad (4)$$

When experimental artifacts are prevented, No and Nw exponents carry important information regarding the rock's wettability, as they define the dynamic behaviour of fluids flow.

The Logbeta is an analytical function used for defining the shape of the capillary pressure versus water saturation curve based on the experimental data.

The Kr and Pc curves are shown in Fig. 14 and Fig. 25.

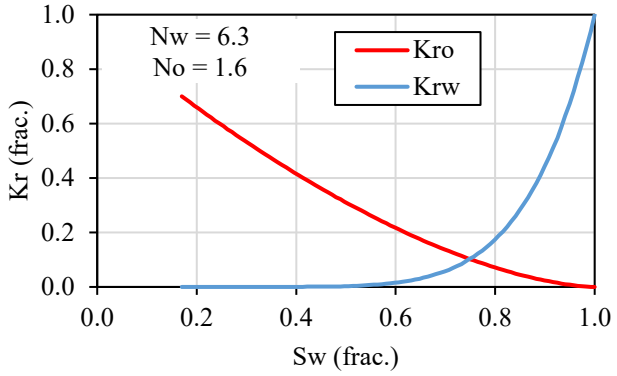

Fig. 25. Computed primary drainage Kr curve for the Richemont sample after optimization of production, dP and Sw profiles.

The experiences described in this paper represent a proof of concept and a validation of the Hybrid Drainage Technique. As this method was conceived to be used on larger samples, generally preferred for SCAL tests, two primary drainage simulations were performed on CYDAR®: one Porous Plate and one HDT. The aim of this test is to compare the experiment duration of both techniques and understand the potential time saving of performing HDT over the Porous Plate on a full-size core. Basic properties, Pc and Kr inputs used for these simulations are presented in Table 4:

Table 4 – Basic, Kr and Pc inputs for CYDAR® simulation

Basic properties	D	50 mm
	L	200 mm
	K_{abs}	2000 mD
	Φ	0.249
	Vp	97.782 cc
Kr	Krw max	0.902
	Kro max	0.800
	Sw min	0.117
	Sw max	1.000
	Nw	5.428
	No	4.792
Pc	Sw min	0.117
	Sw max	1.000
	P_0	7.782 mbar
	$P_{threshold}$	51.469 mbar

Both simulations were performed at inlet pressure equal to 110 mbar and equilibration time for both tests are presented in Fig. 26:

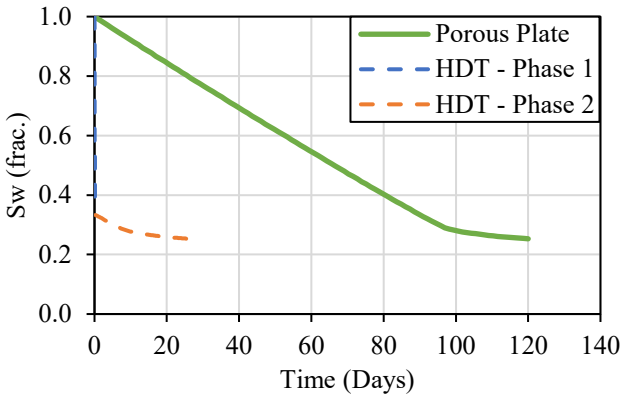

Fig. 26. Comparison between equilibration times for numerical simulations of a conventional Porous Plate and Hybrid Drainage primary drainage.

4 Discussion

Analysis of the HDT imaged by NMR, PP results and saturation profiles from both Centrifuge and Viscous Flooding highlight several important points:

1. The Hybrid Drainage method is effective in eliminating capillary end effects in reduced experimental time compared to a classic PP primary drainage. This has shown to be true in both high and low target Swi on water-wet sandstone and limestone presenting substantially different permeability. This represents a new finding regarding the existing techniques. On the other hand, time reduction appears to be more effective when targeting values of Swi farther from the irreducible water saturation asymptote.

2. In addition, when observing HDT curves for a lower permeability sample (the Richemont case, presented in Fig. 21), it is possible to expect further reduction of the experiment duration as the transition between Phase 1 and Phase 2 could have been performed earlier.

3. The CYDAR® simulation of Porous Plate and HDT on full-size cores agrees with experimental data on smaller plugs. They show that experiment duration reduction is also expected for large SCAL samples.

4. With respect to the saturation profiles obtained in HDT for the Richemont samples, an effect in saturation at the inlet face is observed, which results in a higher MAPE than expected for the saturation profile match. This effect is possibly due to the inlet diffuser format. The diffuser used for these experiments was a classical "bulls-eye", which may concentrate current flow lines bypassing a portion of the inlet face of the sample. Further experiments on a modified-double-spiral diffuser will be performed in order to reduce this effect.

5. Regarding a comparison to the Viscous Flooding method (considered as Phase 1 of the Hybrid Drainage

Technique in this research), the impact on Standard Deviation and "Max-Min" data indicates the effectiveness of the transition to Phase 2 in reducing capillary end effects and producing a homogeneous saturation profile. In addition, as HDT does not remove capillary foot by reversing injection direction, no disconnected oil cluster formation and unwanted imbibition during the primary drainage phase is expected. In Viscous Flooding, this effect has shown to be an obstacle to proper wettability restoration and Kr determination.

6. Moreover, when observing the final saturation profile in Phase 1 for Low Swi – Bentheimer, BEN-HD-LS from Fig. 11, one could state that capillary end effects may have been eliminated by injecting at a higher flowrate. However, this solution is not optimal as this may damage the sample, which could alter its petrophysical properties, such as absolute permeability and porosity, and risk missing the targeted Swi. Using the HDT results in elimination or reduction of the capillary end effects by homogenising the Pc with a porous plate therefore removing any risk of damage to the sample.

7. This methodology has also shown a good agreement when comparing it with the expected fluid dynamics for the first oil flooding from dispersion tests. The Bentheimer samples had a piston-like behaviour and the Richemont samples have shown a much more dispersive shape.

5 Conclusions and perspectives

After analysis of all the experimental data generated by this proof of concept and its advantages and drawbacks, both goals regarding the new method have been attained: 1) the production of a homogeneous saturation profile in 2) a reduced experimental time.

More thorough examination of the results indicates a clear advantage when performing experiments which target higher Swi values; those which have not reached the asymptotic portion of the Pc curve. However, experimental time reduction has been also systematically observed in the lower Swi targets.

As this method has been developed to be applied on Kr experiments, that are generally performed on full-size cores, a test on samples of such dimensions composes one of the next steps of the method's validation. In this case, we expect a greater time saving when comparing to a full-size core Porous Plate primary drainage.

In addition, in order to confirm that the Hybrid Drainage Technique does not induce the generation of disconnect oil clusters during primary drainage, as seen in classic Viscous Oil Flooding, a Hybrid Drainage test imaged by high resolution Micro-tomography will be further performed.

To conclude, a test on reservoir core samples (neutral to oil-wet) may complete the deployment of the method.

6 References

1. C. McPhee, J. Reed and I. Zubizarreta, *Core analysis: a best practice guide*, **vol. 64**, p. 106 (2015)
2. D. Tiab and E. Donaldson, *Petrophysics: theory and practice of measuring reservoir rock and fluid transport properties*, **vol. 3**, p. 47-50 (2012)
3. T.S. Ramakrishnan and A. Cappiello, CES, *A new technique to measure static and dynamic properties of a partially saturated porous medium*, **vol. 46**, p. 1157-1163 (1993)
4. E. J. Fordham, L. D. Hall, T. S. Ramakrishnan, M. R. Sharpe and C. Hall, AICHE journal, *Saturation gradients in drainage of porous media: NMR imaging measurements*, **vol. 39**, no 9, p. 1431-1443 (1993)
5. R. Lenormand, A. Eisenzimmer and C. Zarcone, *A novel method for determination of water/oil capillary pressure of mixed-wettability samples*, SCA1993-22 (1993)
6. D. Huang and M. Honarpour, JPSE, *Capillary end effects in coreflood calculations*, **vol. 19**, p. 103-117 (1998)
7. K. Romanenko and B. Balcom, JPSE, *An assessment of non-wetting phase relative permeability in water-wet sandstones based on quantitative MRI of capillary end effects*, **vol. 110**, p. 225-231 (2013)
8. M. Lombard, S. Gautier, P. Egermann, O. Vizika and E. Tachet, *Petrophysical parameter measurements: comparison of semi-dynamic and centrifuge methods for water-wet and oil-wet limestone samples*, SCA2006-09 (2006)
9. A. Graue, E. Aspenes, T. BOGNØ, R. W. Moe and J. Ramsdal, JPSE, *Alteration of wettability and wettability heterogeneity*, **vol. 33**, p. 3-17 (2002)
10. M. Mascle, S. Youssef, H. Youssef and O. Vizika, *In-situ investigation of ageing protocol effect on relative permeability measurements using high throughput experimentation methods*, SCA2018-016 (2018)
11. D. Green, J. Dick, J. Gardner, B. Balcom and B. Zhou, *Comparison study of capillary pressure curves obtained using traditional centrifuge and magnetic resonance imaging techniques*, SCA2007-30 (2007)
12. M. Fleury, *FRIM: a fast resistivity index measurement method*, SCA1998-29 (1998)
13. P. Faurissoux, A. Colombain, G. Pujol, O. Fraute and B. Nicot, *Ultra Fast Capillary Pressure and Resistivity Index measurements (UFPCRI) combining centrifugation, NMR imaging, and resistivity profiling*, SCA2017-02 (2017)
14. Q. Danielczick, P. Faurissoux and B. Nicot, *Wireless acquisition for Resistivity Index in Centrifuge – Wiri: a new method to estimate Archie's Law parameters*, SCA2021-18 (2021)
15. F. Nono, C. Caubit and R. Rivenq, *Initial states of coreflooding techniques evaluation: a global pore-scale investigation*, SCA2022-T016 (to be published)
16. G. L. Hassler and E. Brunner, AIME 160, *Measurement of capillary pressures in small core samples*, (1945)

17. J. J. Mccullough, F. W. Albaugh and P. H. Jones, DDP, *Determination of the interstitial-water content of oil and gas sand by laboratory tests of core samples*, (1944)
18. M. Fleury, *The Spinning Porous Plate (SSP) method: a new technique for setting irreducible water saturation on core samples*, SCA2009-08 (2009)
19. C. H. Pentland, R. M. El-Maghraby, S. Iglauer and M. J. Blunt, *The toroidal porous plate: a new method to facilitate waterflooding*, SCA2014-068 (2014)
20. B. Satken, H. Bertin and A. Omari, EAGE, *Adsorption/Retention of HPAM polymer in polymer flooding process: effect of molecular weight, concentration and wettability*, p. 1-14, IOR2021-111 (2021)
21. A. T. Corey, *et al.* JPT, *Three-phase relative permeability*, **vol. 8**, no 11, p. 63-65 (1956)